Cover Page

Paper ID: 127

15^{th} International Command and Control Research and Technology Symposium
Santa Monica, California, June 22-24, 2010

"The Evolution of C2"

Sensor Positioning and Selection in Sensor Networks for Target Tracking

Topic:
Modeling and Simulation (Track 6)

UMESH RAMDARAS (PoC)
Combat Systems Department, Netherlands Defence Academy
P.O. Box 10.000, 1780 CA Den Helder, The Netherlands

and

International Research Centre for Telecommunications and Radar, Delft University of Technology
P.O. Box 5031, 2600 GA Delft, The Netherlands
Telephone:+31 223 657019
u.ramdaras@nlda.nl

FRANS ABSIL
Combat Systems Department, Netherlands Defence Academy
P.O. Box 10.000, 1780 CA Den Helder, The Netherlands
fgj.absil@nlda.nl

PIET VAN GENDEREN
International Research Centre for Telecommunications and Radar, Delft University of Technology
P.O. Box 5031, 2600 GA Delft, The Netherlands
p.vangenderen@tudelft.nl

Sensor Positioning and Selection in Sensor Networks for Target Tracking

Umesh Ramdaras [1,2], Frans Absil [1], Piet van Genderen [2]

[1] *Combat Systems Department*
Netherlands Defence Academy
P.O. Box 10.000, 1780 CA Den Helder, The Netherlands
{u.ramdaras,fgj.absil}@nlda.nl

[2] *International Research Centre for Telecommunications and Radar*
Delft University of Technology
P.O. Box 5031, 2600 GA Delft, The Netherlands
p.vangenderen@tudelft.nl

Abstract

Current practice in maritime planning operations is the separation in space and time domain. An adaptive and near real time sensor allocation mechanism would mean a significant step forward towards implementing NEC, and would make better use of the distributed sensor resources.

To realize a NEC systems concept, the coordination between naval units has to increase. The combat management system has to extend its functionality over multiple networked platforms. Sensor management (SM), as part of the C2 loop, has to be automated and applied across ships.

As a step forwards, here we divide automated SM into sensor selection and sensor positioning. The goal is to automatically allocate a network of sensors based on their characteristics. The sensor selection process serves to find the appropriate sensor for doing an observation. Sensor positioning determines the best sensor positions to best deploy the sensor capabilities in the near future. Terminology like 'appropriate' and 'best deployment' imply an optimization process, minimizing a cost function, that acts as the driver mechanism for sensor selection and positioning. As part of the operational picture compilation process, in this paper sensor selection and positioning are applied to optimize the target track accuracy.

1 Introduction

Recent advances in Information and Communication Technology have had their effect on the architecture and the concept of operations (CONOPS) for military systems. Increased connectivity of sensor, weapon and command and control (C2) systems is an enabler for *Network Centric Warfare* (NCW) [Alberts et al., 2000, Cebrowski and Garstka, 1998]. The NCW architecture, essentially a *distributed system*, may be depicted as a cube, containing a layered set of three grids: a sensor, shooter (i.e., weapons) and information grid, with the grid nodes representing individual military systems. The links within and between the grids represent the connectivity.

Introducing such an architecture will have an effect on military operations; this effect is denoted as Network-Enabled Capabilities (NEC). Key NEC characteristics and processes are:

- *multi-sensor data fusion*, i.e., using observations from a multitude of sensor systems to compile an integrated operational picture;
- increased *situational awareness* (SA), i.e., a better understanding of the operational picture in terms of military threats and own capabilities;
- *information superiority*. Through increased connectivity and higher link bandwidths (enabling higher data transfer rates) all parties in the network should have faster and better knowledge of the current battlefield status than an opponent who has no or a less capable network.
- A more rapid C2 loop, also indicated as the *Object-Orient-Decide-Act* loop [Boyd, 1992]. Based on the previous processes and with increased connectivity between Command, Control and Communication (C3) systems, the commander should be able to increase the pace of decision making and keep the momentum on the battlefield. This includes quick assessment of the outcome of the military acts.
- Modernization of the command hierarchy, indicated by terms such as *self synchronization* and delegated authority.

These developments will obviously affect maritime operations. Typical surface ships such as corvettes, frigates and cruisers may contain a suite of sensor systems, dedicated to a specific warfare domain. Radar systems will search, detect and track air and surface objects, while sonars are listening for underwater targets. Typically, electro-optic systems (video, infrared, night vision, etc.) are used near the sea-air interface. Sensor systems may also play a role in the fire control process, when deploying weapon systems. The role of the combat system designer is to integrate the on-board sensor, weapon and C3 systems (the hardware) and implement military capability in the system architecture through a Combat Management System (CMS, the software).

Coordinated system deployment is already an issue on a single ship. Modern, electronically steered radar systems, such as the Thales SMART-L and the APAR on-board of the Royal Netherlands Navy Air Defence and Command Frigate, have the capability to rapidly switch between radar modes or functions, and to adapt the radar settings for each of the modes or functions. Maximizing the benefit from such advanced radar systems requires optimization of their deployment and settings, a process known as *sensor management* (SM). Also coordination between ship, sensor and communication systems is required, e.g., to prevent interference for systems with overlapping frequency ranges.

Moving towards an NCW architecture the coordination between multiple ships, or between ships and other platforms, such as combat aircraft, helicopters or Unmanned Aerial Vehicles (UAVs), will require attention. In a distributed system the optimization process is extended over multiple platforms, each potentially equipped with multiple sensors. Obviously, the degree of complexity increases. Limited coordination between multiple platforms already has been achieved with communication and data link systems (e.g., Link-16, Link-22), where various data types (message, voice, video, etc.) at the tactical or strategic level are shared between units. Also, the concept of Co-operative Engagement Capability, distributing raw radar data between ships, has been tested at sea [Johns Hopkins APL, 1995].

In order to realize the capability of a NCW systems concept the coordination between various naval units will have to be increased. The CMS may have to extend its functionality over multiple platforms, and SM will have to be applied across ships.

In [Bolderheij, 2007] the risk level for relevant military objects in the environment was calculated using a Dynamic Bayesian Network (DBN) approach. This enables threat prioritization and generates sensor task requirements in the sensor manager. Sensor settings will be determined, followed by sensor scheduling (matching sensor resources with demands). The scenario, investigated in the thesis, is an air defense operation of a single ship with a single multi-function radar.

In this paper sensor coordination is extended to a group of moving platforms. A network of maritime radar systems used for air and surface picture compilation will be considered. SM may be divided into *sensor selection* and *sensor positioning*. The outcome of the sensor selection process is the appropriate sensor for doing an observation, while sensor positioning will place the platforms such, that they can best deploy their sensor capabilities in the near future. Terminology like 'appropriate' and 'best deployment' imply an *optimization process*, minimizing a *cost function*, that acts as the driver mechanism for sensor selection and positioning.

With a properly working sensor selection process global sensor deployment (for the entire sensor suite in the network) can be optimized. Suppose that for a given target scenario one is able to identify the best sensor to observe that target within a certain planning horizon, i.e., a number of time intervals ahead, in the meantime the other sensors might be used for other tasks, reducing overlapping observations and redundant sensor measurements. Current practice in maritime operations is space (e.g., allocating search areas or sectors to specific ships in a task group) and time domain separation in the planning stage. An adaptive and near real time sensor allocation mechanism would mean a significant step forward towards implementing NEC, and would make better use of the distributed sensor resources.

1.1 Target Tracking

This work will be limited to the task of *target tracking*, as part of the operational picture compilation process. Target tracking means that a sequence of sensor observations will be used (not necessarily from the same sensor) to estimate the target *state vector*, i.e., a set of attributes characterizing the target. These attributes may include target position (in 3-dimensional space), speed and course, and maneuvers (accelerations). The target state is time-dependent. Therefore, during the tracking process, the state vector will be continuously updated.

The cost function, i.e., the decision metric for SM, is derived from the target state vector. It is a measure for the accuracy in the target state estimate and will contain elements from the *state error covariance matrix*. Which elements will be considered in the cost function may depend on the sensor task, or the stage of a military operation. For a long range surveillance task (e.g., in the range 100-200 km) one is not interested in a highly accurate estimate of target speed and heading; neither is the target altitude highly relevant, so the elevation angle need not be estimated with high precision. An acceptable range and bearing angle will do. If the target is incoming (the outcome of the estimation of the radial velocity component between target object and sensor; an approaching target implies a positive closing speed) a more accurate position, speed and heading estimate will become relevant. If at some point the target turns out to be a (serious) threat, the exact position must be known at each time instant. Now the elevation angle accuracy is as relevant as range and bearing angle accuracy. Before deploying countermeasures one has to make sure that the target is within the operational envelope of defensive weapons. At weapon launch, a guided weapon will need a good estimate of the relative geometry between target and intercepting missile; a gun fired will require a highly accurate estimate of the predicted hitting point of the projectiles (extremely high target position, speed and heading accuracy). In general, the cost function should be a variable, mission-related driver of the sensor selection process.

State estimation is done with the Kalman Filter (KF) [Kalman, 1960,Bar-Shalom and Fortmann, 1988], a first order recursive algorithm with a predictor and a corrector step. It will yield the minimum mean squared error of the state estimate for a linear model (describing the state transition process and the observation process) and assuming zero-mean Gaussian state vector and noise terms (process and measurement noise).

The state transition model describes the target motion. Examples of such models are the constant velocity straight line trajectory and the horizontal turn. The observation model maps the true state space into the observed space. As an observation from a sensor comes in, the processing

will update the predicted state vector. The KF is an iterative algorithm that will yield state estimate updates at each new measurement. This technique is used in many radar tracking applications as target state estimator.

In this paper we have applied the extended KF (EKF) where the state transition and observation models need not be linear functions of the state but may instead be (differentiable) functions.

1.2 Sensor Selection

Sensors obviously have different performance characteristics. Radars may or may not determine the relative target radial velocity component through the Doppler shift measurement. The measurement accuracy might be different for elevation and azimuth angle. One sensor might outperform another in measuring a specific target characteristic. A sensor need not yield an observation, every time it is pointed (looking) at the target; in practice the detection probability $p_d < 1$ and there will be missed detections. Within this research the EKF has been adapted for missed detections in the case of a sensor with $p_d < 1$. The varying sensor performance characteristics have to be incorporated into the SM process.

Selecting a sensor from the sensor grid to perform a task could be done in different ways. It might be carried out randomly (random sensor selection) or with a preference for a certain sensor (fixed sensor selection). In both cases a sensor is selected without taking its suitability into account. On the other hand, sensor selection could be based on prior knowledge or actual performance. In the first case the knowledge, gained from experience in similar situations in the past or from experts, is translated into knowledge networks (e.g., Bayesian Networks [Yilmazer and Osadciw, 2004], Fuzzy Logic [Molina López et al., 1995], etc.). In the second case sensor selection is based on the instantaneous performance measures of the sensors (e.g., error covariance matrix [Ramdaras and Absil, 2006, Chhetri et al., 2003]).

The performance-based sensor selection algorithm (SSA), presented in [Ramdaras and Absil, 2006], compares sensors with respect to the *best expected performance*. For a specific scenario, at each time step within a planning horizon, the sensor with the best expected target attribute accuracy does the observation. E.g., for a good target position estimate sensor selection will be determined by comparing positional variance. Sensor performance evaluation is based on the modified Riccati equation (MRE). In [Boers and Driessen, 2006a, Boers and Driessen, 2006b] it is also shown that the best achievable error performance of the optimal state estimation filter, the Cramér-Rao Lower Bound (CRLB), has an upper bound determined by the solution of the MRE for the class of systems with probability of detection $p_d < 1$. Besides, using the MRE yields a reduced computational load, compared to the CRLB.

In order to investigate the benefits of this MRE SSA, it has been compared to other selection algorithms. In [Ramdaras and Absil, 2006] the MRE SSA is compared to a selection algorithm based on the trace (diagonal elements) of the *updated predicted error covariance matrix* (TRACE SSA) [Chhetri et al., 2003]. In [Ramdaras and Absil, 2007a] results of the comparison of the MRE SSA with a random sensor selection (RSS) and a fixed sensor selection (FSS) scheme are included, while [Ramdaras and Absil, 2007b] presents simulation results for a set of different performance-based selection criteria. In all of these the effect of reduced detection probability of detection was taken into account.

1.3 Sensor Positioning

Target tracking with a radar network can be improved by favorably positioning sensors and selecting the appropriate sensor. Sensor allocation for single target tracking is based on the outcome of the efficient positioning algorithm [Hernandez, 2004] and the MRE SSA using different performance-based selection criteria.

The sensor position one time step ahead is constrained by platform maneuverability (maximum acceleration and heading change). The future sensor position is determined iteratively by the efficient sensor positioning algorithm (SPA). In [Hernandez, 2004] it was shown that the difference between this method and an enumerative positioning method with the same position accuracy constraints is negligible. Besides, the SPA converges much faster and it has less computational requirements. Here, a modified version of the SPA [Hernandez, 2004] is used, dividing the future sensor position envelope in nine sectors instead of four quadrants. In this case a sensor has the possibility to move straight ahead (zero heading change).

However, remember that both sensor selection and positioning may also be bounded by external factors, that have to be taken into account. During a military operation rules of engagement will be in effect (e.g., prohibiting transmissions in certain bearing sectors). There may be geographical constraints or criteria of physical nature (e.g., radar horizon, weather conditions) that limit the positioning and selection procedure.

1.4 Goal and Overview of this Paper

In this paper the goal is to optimize the target track accuracy by first search locally for every sensor the position that will yield the lowest tracking error. Then, based on these best sensor positions, we select that sensor that maximizes the single target track accuracy. Sensor selection at each time yields one composed target track estimate.

We discuss the outcome of a comparison of three sensor positioning cases. We apply the MRE SSA to both stationary co-located sensors and stationary distributed sensors. Furthermore, the MRE SSA and the SPA are used for moving distributed sensors. The MATLAB® computer simulations include three sensors and one target.

The outline of this paper is as follows: in Section 2 the state space representation and measurement models are given. Section 3 presents the MRE SSA and the criteria for sensor selection. In Section 4 the SPA is described. The simulation parameters are given in Section 5. The results are discussed in Section 6, followed by the conclusions and future research topics in Section 7.

2 State Estimation

The simulation uses an x, y orthogonal coordinate system. The data is processed in the discrete time domain $t_k = k\Delta T$, where $\Delta T = 1$ s is the time interval between data points.

There are three radar-type sensors, $s^{(1)}$, $s^{(2)}$ and $s^{(3)}$, each located on a moving platform. The state vector for the j^{th} sensor describes the platform position and speed components in 2-dimensional space

$$\mathbf{x}_s^{(j)} = \begin{bmatrix} x_s^{(j)} & \dot{x}_s^{(j)} & y_s^{(j)} & \dot{y}_s^{(j)} \end{bmatrix}^T. \tag{1}$$

There is one target with a $n_x \times 1$ state vector defined as

$$\mathbf{x} = \begin{bmatrix} x & \dot{x} & y & \dot{y} \end{bmatrix}^T. \tag{2}$$

Target state is estimated using simulated measurement data in polar coordinates (range r, Doppler $\dot{r}$ and bearing θ). Target motion is represented by a state-space process model. This process equation is given by

$$\mathbf{x}_{k+1} = \mathbf{F}\mathbf{x}_k + \mathbf{G}\mathbf{u}_k + \mathbf{v}_k, \tag{3}$$

where $\mathbf{F}$ is the state transition matrix, $\mathbf{G}$ is the input transmission matrix, $\mathbf{u}$ is the (optional) control input vector and $\mathbf{v}$ is the additive process noise, a zero-mean Gaussian process with covariance

matrix $\mathbf{Q} = \mathbf{G}\mathbf{G}^T$ (probability distribution $p(\mathbf{v}) \sim \mathcal{N}(0, \mathbf{Q})$). Since the target motion is described with a constant velocity process model (CVM), $\mathbf{F}$ and $\mathbf{G}$ are

$$\mathbf{F} = \begin{bmatrix} 1 & T & 0 & 0 \\ 0 & 1 & 0 & 0 \\ 0 & 0 & 1 & T \\ 0 & 0 & 0 & 1 \end{bmatrix}, \mathbf{G} = \begin{bmatrix} \frac{1}{2}T^2\sigma_x & 0 \\ T\sigma_x & 0 \\ 0 & \frac{1}{2}T^2\sigma_y \\ 0 & T\sigma_y \end{bmatrix}, \tag{4}$$

where σ_x and σ_y determine the process noise intensity. The measurement model equation for all sensors is given by

$$\mathbf{z}_k^{(j)} = \mathbf{h}^{(j)}(\mathbf{x}_k) + \mathbf{w}_k^{(j)}, \tag{5}$$

where $\mathbf{z}^{(j)}$ is the measurement vector $(n_z^{(j)} \times 1)$ for sensor j, $\mathbf{h}^{(j)}$ is the observer function and $\mathbf{w}^{(j)}$ is the measurement noise, a zero-mean Gaussian process with prior known covariance matrix $\mathbf{R}^{(j)}$ $(p(\mathbf{w}) \sim \mathcal{N}(0, \mathbf{R}^{(j)}))$. Furthermore, the detection probability $0 \leq p_d^{(j)} \leq 1$.

To demonstrate the functioning of the SSA significantly different sensors are defined. $s^{(1)}$ yields bearing information

$$\mathbf{z}_k^{(1)} = \begin{bmatrix} \theta_k \end{bmatrix}^T, \ \mathbf{R}^{(1)} = \begin{bmatrix} \left(\sigma_\theta^{(1)}\right)^2 \end{bmatrix}, \tag{6}$$

$$\mathbf{h}^{(1)}(\mathbf{x}_k) = \begin{bmatrix} \arctan \dfrac{\Delta y_k^{(1)}}{\Delta x_k^{(1)}} \end{bmatrix}, \tag{7}$$

$s^{(2)}$ yields range and bearing information

$$\mathbf{z}_k^{(2)} = \begin{bmatrix} r_k & \theta_k \end{bmatrix}^T, \ \mathbf{R}^{(2)} = \operatorname{diag}\left(\begin{bmatrix} \left(\sigma_r^{(2)}\right)^2 & \left(\sigma_\theta^{(2)}\right)^2 \end{bmatrix}\right), \tag{8}$$

$$\mathbf{h}^{(2)}(\mathbf{x}_k) = \begin{bmatrix} \sqrt{\left(\Delta x_k^{(2)}\right)^2 + \left(\Delta y_k^{(2)}\right)^2} \\ \arctan \dfrac{\Delta y_k^{(2)}}{\Delta x_k^{(2)}} \end{bmatrix}, \tag{9}$$

and $s^{(3)}$ provides range, Doppler and bearing information

$$\mathbf{z}_k^{(3)} = \begin{bmatrix} r_k & \dot{r}_k & \theta_k \end{bmatrix}^T, \ \mathbf{R}^{(3)} = \operatorname{diag}\left(\begin{bmatrix} \left(\sigma_r^{(3)}\right)^2 & \left(\sigma_{\dot{r}}^{(3)}\right)^2 & \left(\sigma_\theta^{(3)}\right)^2 \end{bmatrix}\right), \tag{10}$$

$$\mathbf{h}^{(3)}(\mathbf{x}_k) = \begin{bmatrix} \sqrt{\left(\Delta x_k^{(3)}\right)^2 + \left(\Delta y_k^{(3)}\right)^2} \\ \dfrac{\Delta x_k^{(3)}\dot{x}_k + \Delta y_k^{(3)}\dot{y}_k}{\sqrt{\left(\Delta x_k^{(3)}\right)^2 + \left(\Delta y_k^{(3)}\right)^2}} \\ \arctan \dfrac{\Delta y_k^{(3)}}{\Delta x_k^{(3)}} \end{bmatrix}. \tag{11}$$

In (7), (9) and (11), $\Delta x_k^{(j)}$ and $\Delta y_k^{(j)}$ represent the relative sensor-target geometry

$$\Delta x_k^{(j)} = x_k - x_{k,s}^{(j)}, \ \Delta y_k^{(j)} = y_k - y_{k,s}^{(j)}. \tag{12}$$

Note that for every target state the sensors have different Jacobian matrices $\mathbf{H}^{(j)}$ [Bar-Shalom et al., 2001]

$$\mathbf{H}^{(j)} = \left[\nabla_{\mathbf{x}} \mathbf{h}^{(j)}(\mathbf{x})^T\right]^T. \tag{13}$$

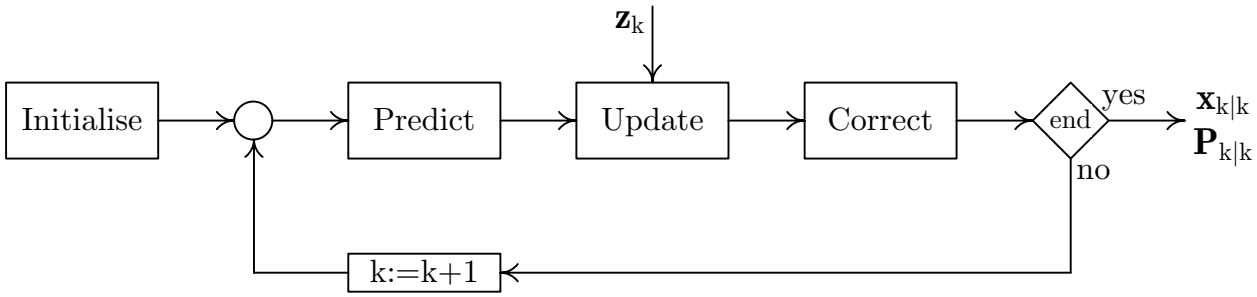

Figure 1: A schematic representation of the EKF for target tracking. For j sensors this algorithm will yield j target tracks.

The Jacobian matrices may be considered as a sensitivity measure; they contain a set of gradients (i.e., partial derivatives) that indicate how a measurement component will change with a variation of a state vector component. At each time step, the Jacobian matrix is evaluated with current predicted state. This process essentially linearizes the non-linear measurement model function around the current estimate.

Target state estimation is performed with the EKF, consisting of the prediction, measurement update and correction steps (see Fig. 1 for a schematic representation). Since $0 \leq p_d^{(j)} \leq 1$, it is possible that no measurement is obtained at a certain time step. In that case the update and correction step are skipped. Target state accuracy (i.e., covariance [Jazwinski, 1970]) is represented by the second moment about the target state. In pseudo-code the KF based algorithm is given by [Bar-Shalom and Li, 1993]:

For $k = 0$ to $k_{\max}$

1. Prediction of the state estimate and error covariance matrix:

$$\mathbf{x}_{k|k-1} = \mathbf{F}\mathbf{x}_{k-1|k-1} + \mathbf{G}\mathbf{u}_{k-1}, \tag{14}$$

$$\mathbf{P}_{k|k-1} = \mathbf{F}\mathbf{P}_{k-1|k-1}\mathbf{F}^T + \mathbf{Q}. \tag{15}$$

2. Prediction of the measurement vector and error covariance matrix:

$$\mathbf{z}_{k|k-1}^{(\hat{j}_k)} = \mathbf{h}^{(\hat{j}_k)}\left(\mathbf{x}_{k|k-1}\right), \tag{16}$$

$$\mathbf{S}_k^{(\hat{j}_k)} = \mathbf{H}_k^{(\hat{j}_k)}\mathbf{P}_{k|k-1}\left(\mathbf{H}_k^{(\hat{j}_k)}\right)^T + \mathbf{R}^{(\hat{j}_k)}, \tag{17}$$

where $\hat{j}_k$ is the selected sensor to obtain the measurement at time step k (see next section).

3. Measurement update (innovation and KF gain). Calculate innovation:

- **If** sensor $\hat{j}_k$ yields a measurement, then

$$\boldsymbol{\nu}_k^{(\hat{j}_k)} = \mathbf{z}_k^{(\hat{j}_k)} - \mathbf{z}_{k|k-1}^{(\hat{j}_k)}, \tag{18}$$

- **Else** (in case of a missed detection)

$$\boldsymbol{\nu}_k^{(\hat{j}_k)} = \mathbf{z}_{k|k-1}^{(\hat{j}_k)} - \mathbf{z}_{k|k-1}^{(\hat{j}_k)} = 0. \tag{19}$$

- **End**

Calculate KF gain:

$$\mathbf{W}_k^{(\hat{j}_k)} = \mathbf{P}_{k|k-1}\left(\mathbf{H}_k^{(\hat{j}_k)}\right)^T\left(\mathbf{S}_k^{(\hat{j}_k)}\right)^{-1}. \tag{20}$$

4. Correction of the state estimate and error covariance matrix:

$$\mathbf{x}_{k|k} = \mathbf{x}_{k|k-1} + \mathbf{W}_k^{(\hat{j}_k)}\boldsymbol{\nu}_k^{(\hat{j}_k)}, \tag{21}$$

$$\mathbf{P}_{k|k} = \left[\mathbf{I} - \mathbf{W}_k^{(\hat{j}_k)}\mathbf{H}_k^{(\hat{j}_k)}\right]\mathbf{P}_{k|k-1}\left[\mathbf{I} - \mathbf{W}_k^{(\hat{j}_k)}\mathbf{H}_k^{(\hat{j}_k)}\right]^T + \mathbf{W}_k^{(\hat{j}_k)}\mathbf{R}^{(\hat{j}_k)}\left(\mathbf{W}_k^{(\hat{j}_k)}\right)^T, \tag{22}$$

where $\mathbf{I}$ is the unit matrix of size $n_x \times n_x$.

5. Increase the time step counter:
$k = k + 1$, and
go to Step 1.

End.

3 Sensor Selection

The sensor selection algorithm (SSA) in [Ramdaras and Absil, 2006] is based on the modified Riccati equation (MRE) given by

$$\hat{\mathbf{P}}_{k+1|k}^{(j)} = \mathbf{F}\mathbf{P}_{k|k-1}\mathbf{F}^T - p_{d,k}^{(j)}\mathbf{F}\mathbf{P}_{k|k-1}\left(\mathbf{H}_k^{(j)}\right)^T\left(\mathbf{H}_k^{(j)}\mathbf{P}_{k|k-1}\left(\mathbf{H}_k^{(j)}\right)^T + \mathbf{R}_k^{(j)}\right)^{-1}\mathbf{H}_k^{(j)}\mathbf{P}_{k|k-1}\mathbf{F}^T + \mathbf{Q}, \tag{23}$$

where $\hat{\mathbf{P}}_{k+1|k}^{(j)}$ is the expected performance at time step $k+1$ for sensor j, $\mathbf{P}_{k|k-1}$ is the predicted state error covariance matrix, $p_{d,k}^{(j)}$ is the probability of detection and $\mathbf{H}_k^{(j)}$ is the Jacobian of the measurement matrix using the state estimate for the linearization process. Observe that in (23) the sensor properties are included in $p_{d,k}^{(j)}$ and the measurement accuracy $\mathbf{R}_k^{(j)}$. In the rest of this paper we will consider both parameters as time-independent (i.e., $p_d^{(j)}$ and $\mathbf{R}^{(j)}$). Also, for every sensor the current target state, and therefore the current geometry is represented in this equation by $\mathbf{H}_k^{(j)}$.

Criteria for sensor selection are based on considering specific elements from $\hat{\mathbf{P}}_{k+1|k}^{(j)}$ and minimizing a cost function $C_k^{(j)}$. In [Ramdaras and Absil, 2006] the sensor selection criterion is the best expected target position accuracy (i.e., minimum positional variance in x and y, as expressed by σ_{xx}^2, σ_{xy}^2 and σ_{yy}^2) and therefore the cost function is defined as

$$C_k^{(j)} = \det\begin{pmatrix} \hat{\mathbf{P}}_{k+1|k}^{(j)}(1,1) & \hat{\mathbf{P}}_{k+1|k}^{(j)}(1,3) \\ \hat{\mathbf{P}}_{k+1|k}^{(j)}(3,1) & \hat{\mathbf{P}}_{k+1|k}^{(j)}(3,3) \end{pmatrix} = \det\begin{pmatrix} \hat{\sigma}_{xx}^2 & \hat{\sigma}_{xy}^2 \\ \hat{\sigma}_{xy}^2 & \hat{\sigma}_{yy}^2 \end{pmatrix}. \tag{24}$$

In [Ramdaras and Absil, 2007b] four alternative selection criteria are considered: best expected heading, range, Doppler and bearing accuracy. In that case the cost function is expressed as [Zwaga and Driessen, 2005]

$$C_k^{(j)} = \mathbf{H}^c\left(\hat{\mathbf{x}}_{k|k-1}\right)\hat{\mathbf{P}}_{k+1|k}^{(j)}\mathbf{H}^c\left(\hat{\mathbf{x}}_{k|k-1}\right)^T, \tag{25}$$

where $\hat{\mathbf{x}}_{k|k-1}$ is the predicted target state vector and $\mathbf{H}^c$ is one of the four cases given in (26). For convenience, the subscript $k|k-1$ of the elements of $\hat{\mathbf{x}}_{k|k-1}$ is omitted in (26) and $r = \sqrt{x^2+y^2}$.

$$\mathbf{H}^c\left(\hat{\mathbf{x}}_{k|k-1}\right) = \begin{cases} \left[\begin{array}{cccc} 0 & -\dfrac{\dot{y}}{\dot{x}^2+\dot{y}^2} & 0 & \dfrac{\dot{x}}{\dot{x}^2+\dot{y}^2} \end{array}\right] & \text{for heading,} \\ \left[\begin{array}{cccc} \dfrac{x}{r} & 0 & \dfrac{y}{r} & 0 \end{array}\right] & \text{for range,} \\ \left[\begin{array}{cccc} \dfrac{\dot{x}}{r} - \dfrac{x^2\dot{x}+xy\dot{y}}{r^3} & \dfrac{x}{r} & \dfrac{\dot{y}}{r} - \dfrac{xy\dot{x}+y^2\dot{y}}{r^3} & \dfrac{y}{r} \end{array}\right] & \text{for Doppler,} \\ \left[\begin{array}{cccc} -\dfrac{y}{r^2} & 0 & \dfrac{x}{r^2} & 0 \end{array}\right] & \text{for bearing/azimuth.} \end{cases} \tag{26}$$

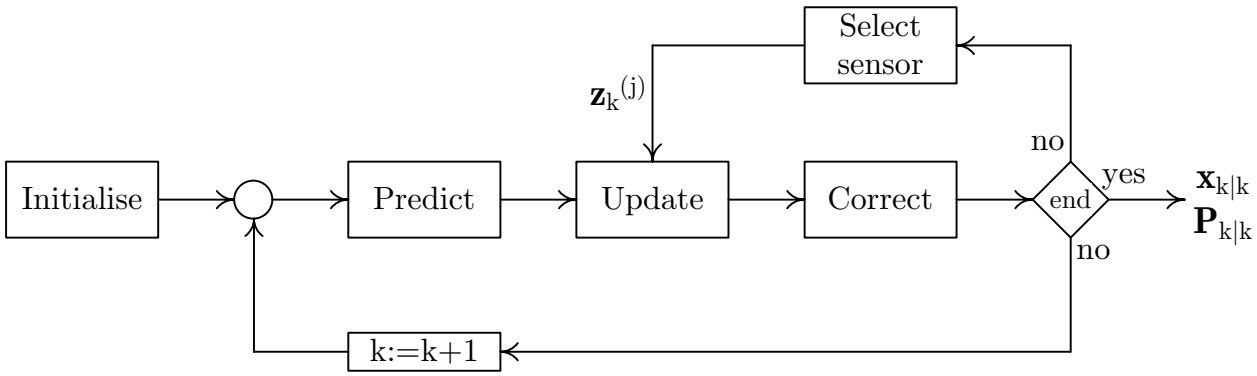

Figure 2: A schematic representation of the MRE SSA, represented by the sensor selection block, in relation to the target tracking algorithm. Note that j sensors will yield one target track.

The optimal sensor $\hat{j}_k$ at time step k is selected by minimizing the cost function as

$$\hat{j}_k = \arg\min \left\{ C_k^{(j)} \right\}, \; j = 1 : j_{\max}. \tag{27}$$

Fig. 2 shows a schematic representation of the MRE SSA, represented by the sensor selection block, in relation to the target tracking algorithm. In contrast with Fig. 1, this algorithm will yield only one target trajectory, composed of measurements by multiple sensors.

In Fig. 3 the MRE SSA is schematically depicted. Based on the the predicted error covariance matrix and the sensor-dependent parameters, the expected performance is computed for each sensor (see (23)). Then, the costs are computed with (25) for a certain selection criterion. The sensor that minimizes these costs, according to (27), is selected to obtain a measurement at time k.

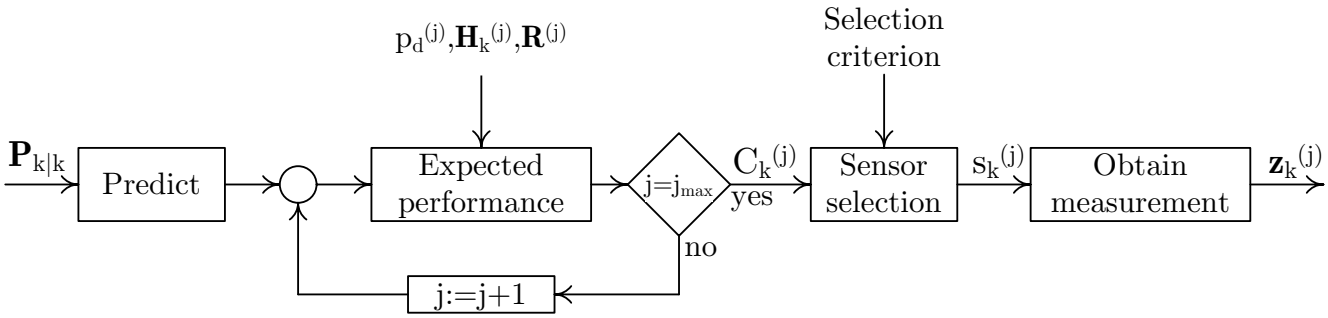

Figure 3: A schematic representation of the MRE SSA. For every sensor the expected performance is computed. Based on a selection criterion, the sensor that minimizes the cost function is selected to obtain a measurement at time k.

4 Sensor Positioning

The sensor position one time step ahead is constrained by the platform speed v and maneuverability (maximum possible longitudinal acceleration a and heading change α). The future sensor position envelope is divided into nine sectors (see Fig. 4). Over $d_{\max}$ iterative steps, one of the sectors is subdivided into nine smaller segments, based on best expected performance, i.e., minimization of the target state error covariance matrix. The desired sensor position accuracy will determine the number of iteration steps.

For each corner point the cost is computed based on the MRE expected performance. The sector that minimizes the total costs (i.e., the added costs at the four corner points) will be selected. When $d_{\max}$ is reached, the geometric center of the last selected sector is the future sensor position $\hat{\mathbf{x}}^{(j)}_{k|k-1,s}$. $\mathbf{x}_{k|k-1}$ and $\hat{\mathbf{x}}^{(j)}_{k|k-1,s}$ are used to obtain $\mathbf{H}^{(j)}_{k|k-1}$ according to (13).

$\mathbf{H}^{(j)}_{k|k-1}$ and $\mathbf{P}_{k|k-1}$ are used as input to compute the expected performance for the different sensors. Based on the selection criterion a sensor is selected to perform the measurement at time step k. Once this measurement is obtained, the tracking algorithm continues with the update step (innovation and gain computation).

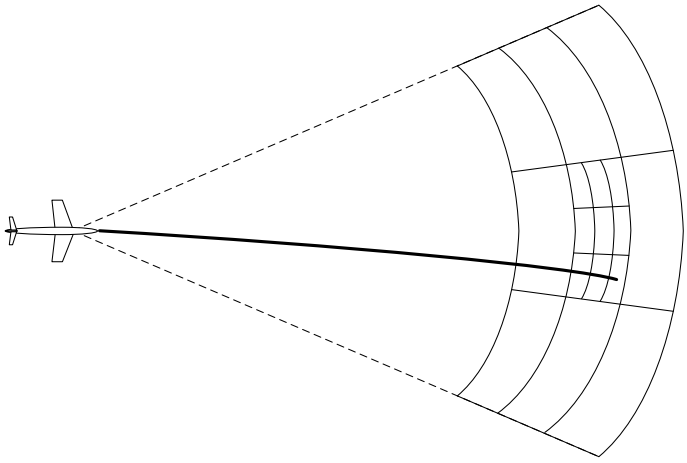

Figure 4: The future sensor position envelope is divided into nine sectors. This envelope is constrained by the platform maneuverability (maximum possible acceleration) and heading change. Here, two iteration steps are depicted.

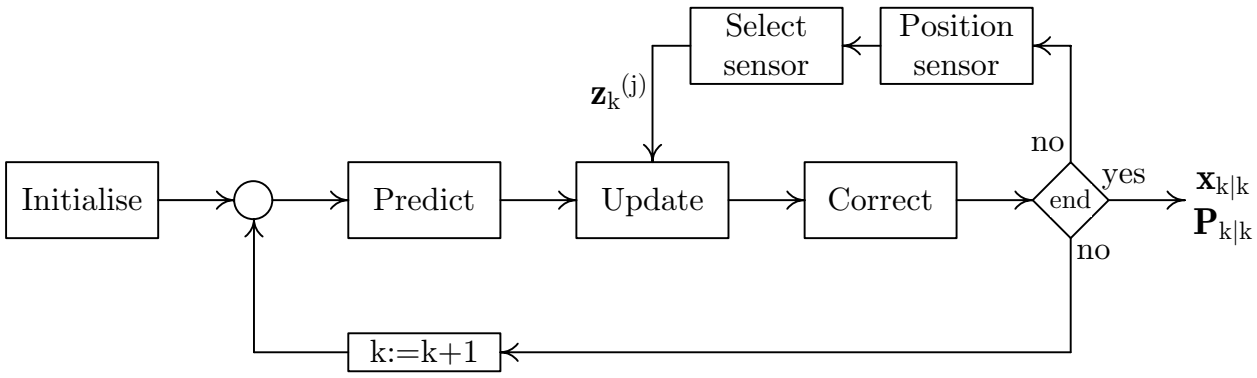

Figure 5: A schematic representation of the SPA and MRE SSA, represented by the sensor positioning and sensor selection blocks, respectively, in relation to the target tracking algorithm. First, the SPA will search for the best sensor positions, then the best available sensor is selected to obtain the measurement at time k.

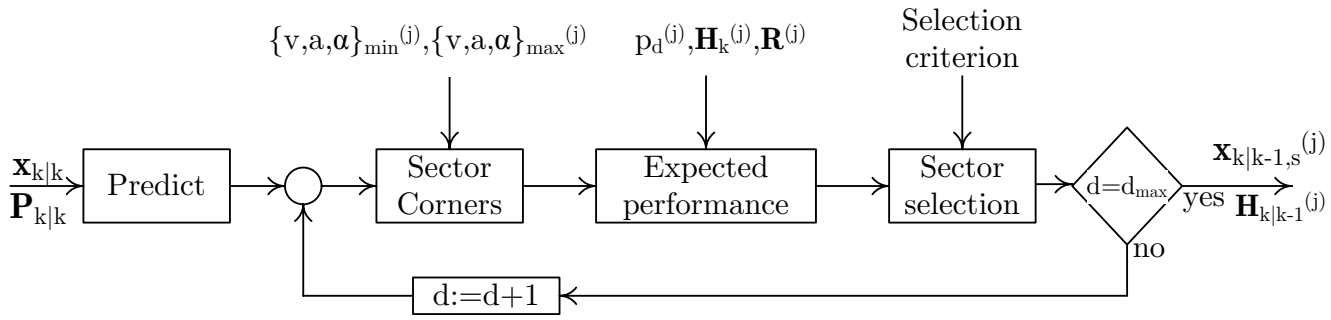

Figure 6: A schematic representation of the SPA. For every sensor the future positional envelope is computed and divided into 9 sectors. The sector that minimises the MRE-based cost function is selected and divided again into 9 sectors, until $d_{\max}$ is reached.

In the upper part of Fig. 5 the SPA and the MRE SSA are shown. First, we search for every sensor the best future position that will minimize the target track error (i.e., a local optimizing process). Then, based on these best sensor positions, the sensor is selected that will maximize the target track accuracy (i.e., a global optimizing process).

In Fig. 6 a schematic representation of the SPA is depicted. For every sensor the future position envelope is computed and divided into 9 sectors. The sector that minimizes the MRE-based cost function is selected and divided again into 9 sectors, until $d_{\max}$ is reached. From the predicted sensor position we extract $\mathbf{H}_{k|k-1}^{(j)}$, which is an input for the MRE SSA.

It is reasonable to use the same selection criterion for both the SPA and the MRE SSA, since both algorithms optimize the target accuracy for this specific criterion.

5 Simulation Parameters

We consider a 2-dimensional geometry with an area (top view) of 13×13 km^2. The simulation includes three single radar-like sensor moving platforms ($s^{(1)}$, $s^{(2)}$ and $s^{(3)}$, with performance parameters (6) to (11)) and one CVM opening target (see Fig. 7 for the true target trajectory). The total duration of the scenario is $k_{\max} = 100$ s.

To demonstrate the benefits of the MRE SSA and the SPA we will consider three sensor positioning cases:

- Case 1: Co-located sensors stationary position at either $(0, 0)$ km, $(3, 9)$ km or $(10, 8)$ km. These positions are selected in an arbitrary way.
- Case 2: Distributed sensor network with $s^{(1)}$ at $(9, 4)$ km, $s^{(2)}$ at $(4, 8)$ km and $s^{(3)}$ at $(4, 2)$ km.
- Case 3: Positioning based on the SPA with $d_{\max} = 5$ and the best expected position accuracy criterion.

In all these cases the best expected position accuracy criterion (see (24)) is used for sensor selection.

Performance evaluation is based on $\det\left(\mathbf{P}_{k|k}\right)_{pos}$, i.e., the determinant of the positional variance elements of the corrected error covariance matrix $\mathbf{P}_{k|k}$ ($\mathbf{P}_{k|k}$ is obtained with (22)).

The three sensors have different measurements accuracies

$$\mathbf{R}^{(1)} = \mathrm{diag}\left[\begin{array}{c} 2.47 \times 10^{-6} \end{array}\right],$$
$$\mathbf{R}^{(2)} = \mathrm{diag}\left[\begin{array}{cc} 1000 & 2.47 \times 10^{-6} \end{array}\right],$$
$$\mathbf{R}^{(3)} = \mathrm{diag}\left[\begin{array}{ccc} 60 & 100 & 2.47 \times 10^{-4} \end{array}\right].$$

$s^{(1)}$ yields only good bearing measurements ($\sigma_\theta^{(1)} = \sqrt{2.47 \times 10^{-6}}$ rad $= 0.09°$). $s^{(2)}$ has the same bearing accuracy as $s^{(1)}$, while the range accuracy is poor ($\sigma_r^{(2)} = 31.6$ m). $s^{(3)}$ yields good range and Doppler information ($\sigma_r^{(3)} = 7.7$ m, $\sigma_{\dot{r}}^{(3)} = 10$ m/s), but poor bearing accuracy ($\sigma_\theta^{(3)} = 0.9°$).

The detection probability is assumed to be fixed during these simulations, $p_d^{(1)} = p_d^{(2)} = p_d^{(3)} = 1$, but in a more complex scenario it could be time-dependent.

Initial target state vector and error covariance matrix are

$$\mathbf{x}_{0|0} = \begin{bmatrix} 1000 & 100 & 1000 & 100 \end{bmatrix}^T,$$
$$\mathbf{P}_{0|0} = \text{diag}\begin{bmatrix} 100 & 10 & 100 & 10 \end{bmatrix},$$

respectively, and $\sigma_x = \sigma_y = 5$ m (process noise intensity).

For Case 3, the platform initial states are

$$\mathbf{x}_{0|0,s}^{(1)} = \begin{bmatrix} 9000 & -75 & 4000 & 0 \end{bmatrix}^T.$$
$$\mathbf{x}_{0|0,s}^{(2)} = \begin{bmatrix} 4000 & -75 & 8000 & 0 \end{bmatrix}^T.$$
$$\mathbf{x}_{0|0,s}^{(3)} = \begin{bmatrix} 4000 & 0 & 2000 & 75 \end{bmatrix}^T.$$

The platforms have a minimum speed of 50 m/s and a maximum speed of 200 m/s. Their maximum acceleration and heading change are 10 m/s^2 and $\pi/20$ rad/s, respectively.

6 Simulation Results

In the first part of this section the MRE SSA is applied to co-located stationary sensors at three different positions. In the second part target tracking with a distributed sensor network is considered and the performance is compared with the performance of Case 1. The MRE SSA is used for both stationary and moving distributed sensors. Sensor motion is based on the SPA.

6.1 Co-located Stationary Sensors at Three Different Positions

In Fig. 7 the true target trajectory is depicted as well as the three co-located stationary sensor positions for Case 1. The true target trajectory is not a straight line, due to the added process noise $\mathbf{v}$. From those three positions we will apply sensor selection.

The sensor selection strategies for Case 1 are given in Fig. 8. Since $s^{(1)}$ and $s^{(2)}$ are co-located, $s^{(1)}$ is not selected during the entire trajectory ($\sigma_\theta^{(1)} = \sigma_\theta^{(2)}$, but $s^{(2)}$ yields additional range information). The sensor preference alternates between $s^{(2)}$ and $s^{(3)}$ to reduce $\det\left(\mathbf{P}_{k|k}\right)_{pos}$. One time step $s^{(2)}$ yields good bearing angle updates and reduces the error covariance matrix in the cross-range direction, while the next time step $s^{(3)}$ yields good range and Doppler information to reduce the error covariance matrix in the range direction. Notice that this selection strategy holds for all co-located sensor positions of Case 1, since the relative position between $s^{(1)}$ or $s^{(2)}$ on the one hand and $s^{(3)}$ on the other hand is always the same. In these cases the line-of-sight (LOS) angle between the sensors and the target is the same. An alternating preference for either $s^{(1)}$ or $s^{(2)}$ and then $s^{(3)}$ is the optimal selection strategy to minimize $\det\left(\mathbf{P}_{k|k}\right)_{pos}$.

In Fig. 9 the $\det\left(\mathbf{P}_{k|k}\right)_{pos}$ is shown for all three positions. For the sensors placed at $(0, 0)$ km we notice that $\det\left(\mathbf{P}_{k|k}\right)_{pos}$ increases due to the increasing distance between the sensors and the target. The $\det\left(\mathbf{P}_{k|k}\right)_{pos}$ will decrease for a closing target, i.e., for sensors placed at $(10, 8)$ km. Also, observe a decrease of $\det\left(\mathbf{P}_{k|k}\right)_{pos}$ for sensors positioned at $(3, 9)$ km for $t = 0 - 50$ s, after which time there is an increase due to the opening target.

So, although the sensor parameters and selection strategies are the same for all three co-located sensor positions, the performance measure strongly depends on the sensor position.

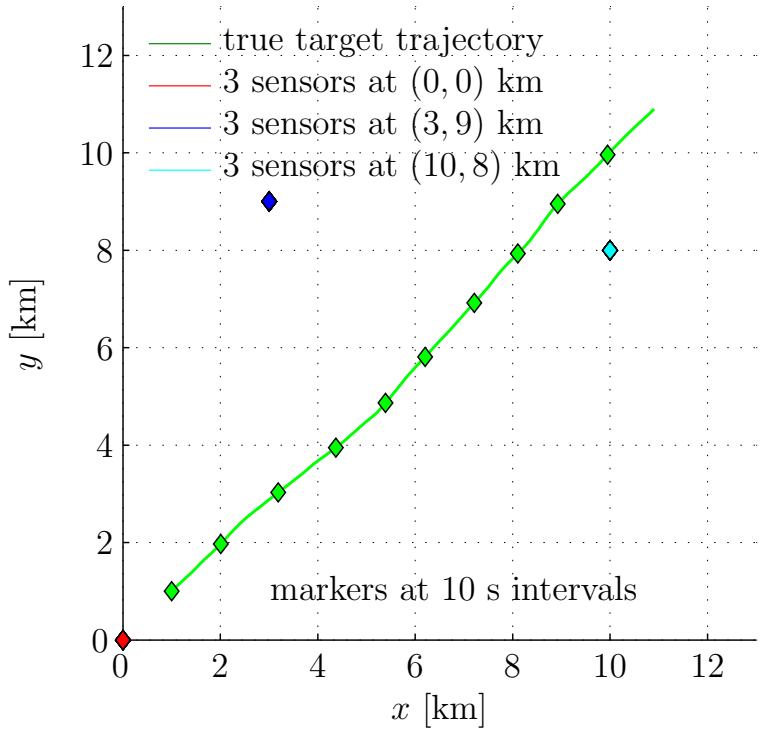

Figure 7: The opening true target track (with respect to $(0,0)$) and three co-located sensors positions for Case 1.

6.2 Stationary and Moving Distributed Sensors

In Fig. 10 the co-located stationary sensors are placed at $(3,9)$ km (Case 1). The initial positions of the distributed sensors of Case 3 are the same as the stationary sensor positions for Case 2. For Case 3 the sensor trajectories are shown.

Note that for Case 3 the future position of a sensor also depends on the past performance of the other sensors. After all, based on the measurement of the selected sensor and its parameters (the measurement accuracies in $\mathbf{R}$ and the p_d), the obtained $\mathbf{P}_{k|k}$ is an input of the SPA (see Figs. 5-6). E.g., if $s^{(3)}$ yields an observation at $t = 40$ s its measurement performance will influence $\mathbf{P}_{40|40}$. It will have a good accuracy in the range direction, but the cross-range accuracy is poor. Based on this corrected covariance matrix the best sensor positions at $t = 41$ s are computed. The future sensor positions might be different if another sensor had been selected at $t = 40$ s.

Observe that all sensors start moving towards the target. Then, they cross the target trajectory and try to catch up with the target.

In Fig. 11 the sensor selection strategies are given for all three positioning cases. The selection strategy of Case 1 is already discussed. For Case 2 and Case 3, where the sensors are not co-located, the LOS-angle between the sensors and the target is not the same. Now, in general, that sensor will be selected that alternates with $s^{(3)}$ and has the smallest LOS-angle difference with $s^{(3)}$. For Case 3 a same reasoning holds, only now the sensor positions change every time step.

Fig. 12 depicts $\det\left(\mathbf{P}_{k|k}\right)_{pos}$ for all three cases. The two humps of the $\det\left(\mathbf{P}_{k|k}\right)_{pos}$ for Case 2 (between $t = 16 - 20$ s and $t = 47 - 51$ s) are due to multiple successive selections of $s^{(3)}$. The hump for Case 3 between $t = 30 - 55$ s is due to the increasing distance between $s^{(3)}$ and the target. Compared to and Case 2, we can conclude that Case 3 yields the lowest $\det\left(\mathbf{P}_{k|k}\right)_{pos}$. Furthermore, stationary distributed sensors do not necessarily yield better performance compared to co-located sensors. If we would compare the performance of Case 2 with Case 1 where the 3 sensors are at $(0,0)$ km, the distributed sensors would have yielded a better performance (not shown here).

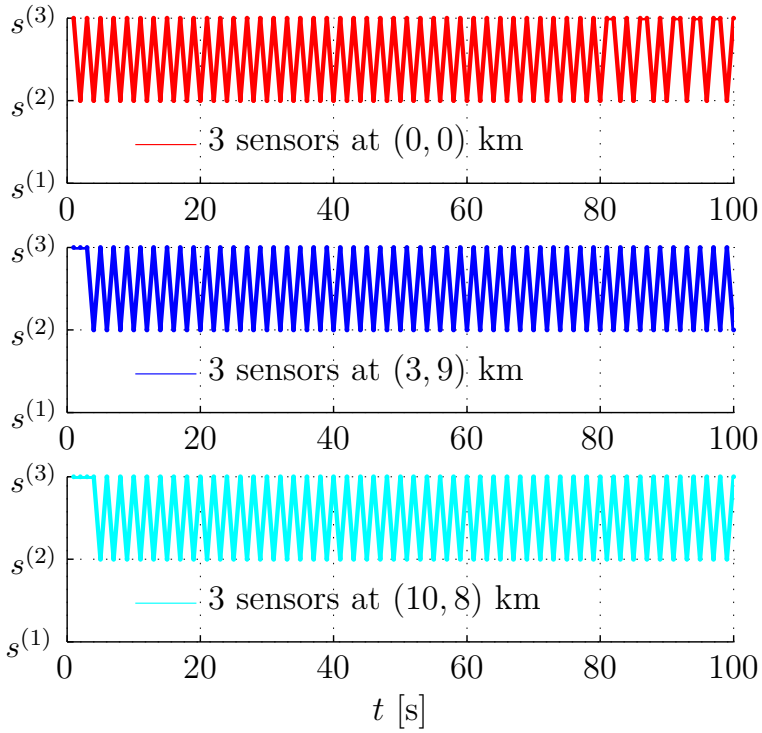

Figure 8: The sensor selection strategies for all three co-located non-moving sensor positions of Case 1. Sensor selection is performed with the MRE SSA and the best expected target position accuracy criterion.

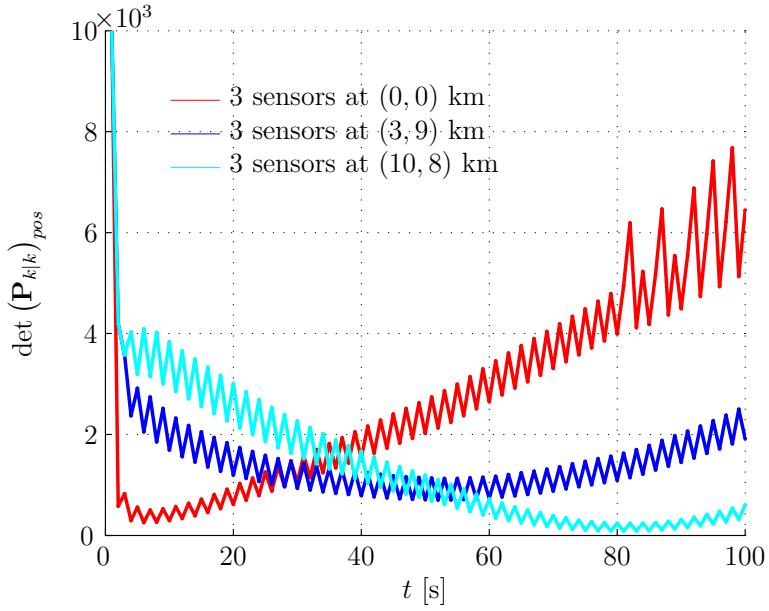

Figure 9: The determinant of the positional variance elements of the corrected error covariance matrix $\mathbf{P}_{k|k}$ for all three co-located non-moving sensor positions of Case 1. Sensor selection is performed with the MRE SSA and the best expected target position accuracy criterion.

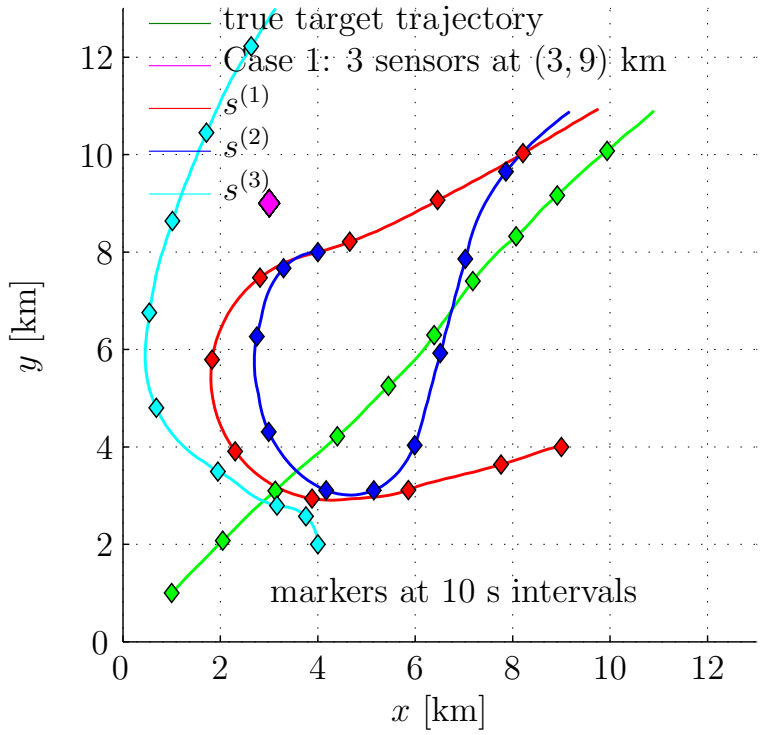

Figure 10: The true target track and sensor positions for all three cases. For Case 1 the sensors are placed at $(3, 9)$ km. For Case 2 $s^{(1)}$, $s^{(2)}$ and $s^{(3)}$ are placed at $(9, 4)$ km, $(4, 8)$ km and $(4, 2)$ km, respectively. The initial sensor positions of Case 3 are the same as for Case 2. Sensor positioning for Case 3 is based on the SPA.

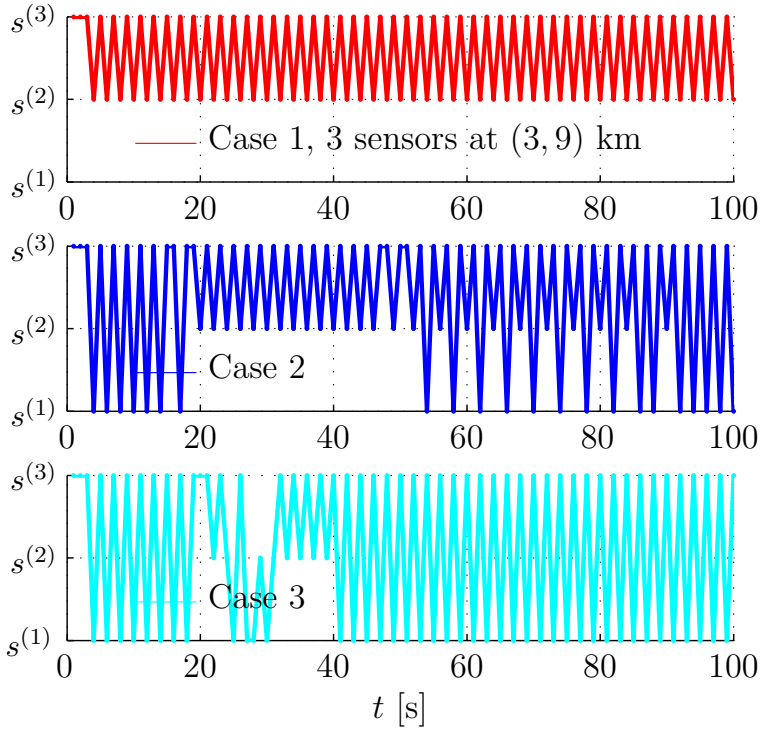

Figure 11: The sensor selection strategies for all three sensor positioning cases. Sensor selection is performed with the MRE SSA and the best expected target position accuracy criterion.

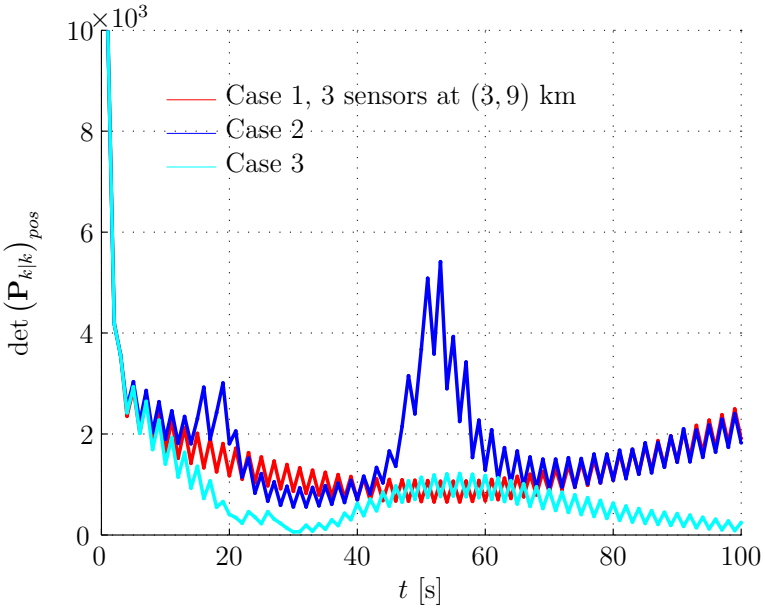

Figure 12: The determinant of the positional variance elements of the corrected error covariance matrix $\mathbf{P}_{k|k}$ for all sensor positioning cases. Sensor selection is performed with the MRE SSA and the best expected target position accuracy criterion.

7 Conclusions and Future Research Topics

In this paper we have used a combination of a sensor positioning algorithm (SPA) and sensor selection algorithm (SSA) for minimizing the target track error. Sensor positioning is based on an efficient algorithm (fast convergence, combined with reduced computational requirements).

The outcome of both the SPA and the SSA is based on the expected target state accuracy, computed with the modified Riccati equation (MRE). The cost function enables a combination of the expected sensor performance and various selection criteria. In this paper for both algorithms we have applied the best expected target position accuracy criterion. Single target tracking is performed with the extended Kalman filter and three sensors are used. Performance evaluation is based on the determinant of the positional variance elements of the corrected error covariance matrix.

Three positioning cases are simulated: stationary co-located sensors (at three positions), stationary distributed sensors and sensors determining their future best position based on the SPA and the positioning criterion.

For the scenarios simulated here, the results show that the combination of sensor positioning with the SPA and the best expected position accuracy criterion and sensor selection with the same criterion yields the best performance compared to the other cases.

In general, for our sensor selection scenarios, the preference alternates between a sensor with good range and Doppler measurements, but a poor bearing accuracy and a sensor with a good bearing accuracy, but poor or no range measurements. The determinant of the positional variance elements of the corrected error covariance matrix is minimized when the sensors have the same (or a small difference in) line-of-sight-angle between sensor and target.

In this paper we have used a simplified scenario to demonstrate the performance of the combination of the SPA and the MRE SSA. In more realistic scenarios the future sensor position depends on various parameters (e.g., varying sensor platform maneuverability parameters, probability of detection, etc.). Although not yet proven mathematically, the prospect is that the combination of SPA and MRE SSA will yield the best performance (based on the outcome of the simulations in

this paper).

Future research may focus on aspects like multiple time steps ahead sensor position planning (here the planning horizon is limited to one time step ahead), the influence of the prediction model in case of a longer planning horizon (in this paper a constant velocity model is used) or the behavior of sensors when multiple targets are involved (here one target is considered).

References

[Alberts et al., 2000] Alberts, D., Garstka, J., and Stein, F. (2000). *Network Centric Warfare: Developing and Leveraging Information Superiority*. CCPR Publication Series, 2nd edition.

[Bar-Shalom and Fortmann, 1988] Bar-Shalom, Y. and Fortmann, T. (1988). *Tracking and Data Association*. Academic Press, New York.

[Bar-Shalom and Li, 1993] Bar-Shalom, Y. and Li, X. (1993). *Estimation and Tracking: Principles, Techniques, and Software*. Artech House, Inc.

[Bar-Shalom et al., 2001] Bar-Shalom, Y., Li, X., and Kirubarajan, T. (2001). *Estimation with Applications to Tracking and Navigation: Theory, Algorithms and Software*. John Wiley & Sons, Inc.

[Boers and Driessen, 2006a] Boers, Y. and Driessen, H. (2006a). On the Modified Riccati Equation and its Application to Target Tracking. *IEE Proceedings - Radar, Sonar and Navigation*.

[Boers and Driessen, 2006b] Boers, Y. and Driessen, H. (2006b). Results on the Modified Riccati Equation: Target Tracking Applications. *IEEE Transactions on Aerospace and Electronic Systems*, 42(1):379–384.

[Bolderheij, 2007] Bolderheij, F. (2007). *Mission-Driven Sensor Management: Analysis, Design, Implementation and Simulation*. PhD thesis, Delft University of Technology.

[Boyd, 1992] Boyd, J. (1987-1992). A Discource on Winning and Losing. Unpublished briefing notes, available at: `http://www.d-n-i.net/richards/boyds_ooda_loop.ppt`.

[Cebrowski and Garstka, 1998] Cebrowski, K. and Garstka, J. (1998). Network-Centric Warfare: Its Orgin and Future. *Proceedings of the Naval Institute*, 124(1):28–35.

[Chhetri et al., 2003] Chhetri, A., Morrell, D., and Papandreou-Suppappola, A. (2003). Scheduling Multiple Sensors Using Particle Filters in Target Tracking. *IEEE Proceedings of the Statistical and Signal Processing Workshop*.

[Hernandez, 2004] Hernandez, M. (2004). Optimal Sensor Trajectories in Bearing-Only Tracking. *Proceedings of the Seventh International Conference on Information Fusion*.

[Jazwinski, 1970] Jazwinski, A. (1970). *Stochastic Processes and Filtering Theory*, volume 64 of *Mathematics in Science and Engineering*. Academic Press, Inc.

[Johns Hopkins APL, 1995] Johns Hopkins APL (1995). The Cooperative Engagement Capability. *Johns Hopkins APL Technical Digest*, 16(4):377–396.

[Kalman, 1960] Kalman, R. (1960). A New Approach to Linear Filtering and Prediction Problems. *Transactions of the ASME - Journal of Basic Engineering*, 82:35–45.

[Molina López et al., 1995] Molina López, J., Jiménez Rodríquez, F., and Casar Corredera, J. (1995). Fuzzy Reasoning for Multisensor Management. *Proceedings of the IEEE Conference on Systems, Man and Cybernetics: "Intelligent Systems for the 21st Century"*, 2:1398–1403.

[Ramdaras and Absil, 2006] Ramdaras, U. and Absil, F. (2006). Networks of Maritime Radar Systems: Sensor Selection Algorithm for $P_d < 1$ Based on the Modified Riccati Equation. *Proceedings of the IEEE Nonlinear Statistical Signal Processing Workshop: Classical, Unscented and Particle Filtering Methods*.

[Ramdaras and Absil, 2007a] Ramdaras, U. and Absil, F. (2007a). Sensor Selection: the Modified Riccati Equation Approach Compared with other Selection Schemes. *Proceedings of the Tenth International Conference on Information Fusion*.

[Ramdaras and Absil, 2007b] Ramdaras, U. and Absil, F. (2007b). Target Tracking in Sensor Networks: Criteria for Sensor Selection. *Proceedings of the IEEE Radar Conference*, pages 192–196.

[Yilmazer and Osadciw, 2004] Yilmazer, N. and Osadciw, L. (2004). Sensor Management and Bayesian Networks. *Proceedings of SPIE – Multisensor, Multisource Information Fusion: Architectures, Algorithms, and Applications*, 5434:238–248.

[Zwaga and Driessen, 2005] Zwaga, J. and Driessen, H. (2005). Tracking Performance Constrained MFR Parameter Control: Applying Constraints on Prediction Accuracy. *Proceedings of the Eighth International Conference on Information Fusion*, pages 546–551.